THE JOURNAL OF BIOLOGICAL CHEMISTRY VOL. 281, NO. 26, pp. 18135–18144, June 30, 2006
Printed in the U.S.A.

Complete Structures of *Bordetella bronchiseptica* and *Bordetella parapertussis* Lipopolysaccharides*

Received for publication, December 30, 2005, and in revised form, April 21, 2006 Published, JBC Papers in Press, April 21, 2006, DOI 10.1074/jbc.M513904200

Andrew Preston‡, Bent O. Petersen§, Jens Ø. Duus§, Joanna Kubler-Kielb¶, Gil Ben-Menachem¶, Jianjun Li‖, and Evgeny Vinogradov‖1

From the ‖Institute for Biological Sciences, National Research Council, Ottawa, Ontario K1A OR6, Canada, ‡Department of Molecular and Cellular Biology, University of Guelph, Guelph, Ontario N1G 2W1, Canada, §Carlsberg Laboratory, DK 2500 Valby Copenhagen, Denmark, and ¶NICHD, National Institutes of Health, Bethesda, Maryland 20892

The structures of the lipopolysaccharide (LPS) core and O antigen of *Bordetella bronchiseptica* and *Bordetella parapertussis* are known, but how these two regions are linked to each other had not been determined. We have studied LPS from several strains of these microorganisms to determine the complete carbohydrate structure of the LPS. LPS was analyzed using different chemical degradations, NMR spectroscopy, and mass spectrometry. This identified a novel pentasaccharide fragment that links the O chain to the core in all the LPS studied. In addition, although the O chain of these bacteria was reported as a homopolymer of 1,4-linked 2,3-diacetamido-2,3-dideoxy-α-galacturonic acid, we discovered that the polymer contains several amidated uronic acids, the number of which varies between strains. These new data describe the complete structure of the LPS carbohydrate backbone for both *Bordetella* species and help to explain the complex genetics of LPS biosynthesis in these bacteria.

The genus *Bordetella* currently comprises nine species of Gram-negative bacteria. The most extensively studied of these are the respiratory pathogens *B. pertussis*, *B. parapertussis*, and *B. bronchiseptica*. *B. pertussis* infects only humans and is the causative agent of whooping cough in infants and persistent respiratory infections in adults (1). *B. parapertussis* exists as two separate lineages. One is adapted to the human host and causes whooping cough; the other is adapted to the ovine host in which it can cause chronic pneumonia (2). In contrast, *B. bronchiseptica* colonizes the respiratory tract of a large number of animals, and although it causes respiratory infections in some farm, companion, and wild animals, most *B. bronchiseptica* infections are asymptomatic and chronic. *B. bronchiseptica* is occasionally isolated from the respiratory tract of humans and is likely acquired through contact with infected animals (3, 4). Although these three pathogens are very closely related genetically (5), they synthesize different lipopolysaccharide (LPS)[2] molecules. All three LPS share similar lipid A and core structures (6), yet only *B. parapertussis* and *B. bronchiseptica* synthesize O antigens. Initially, the O antigens of both species were reported to be identical and composed of linear polymers of 1,4-linked 2,3-diacetamido-2,3-dideoxy-α-galacturonic acid (7), but later differences between the end groups on *B. bronchiseptica* O antigens were described (8). The core oligosaccharides of *B. pertussis* and *B. bronchiseptica* possess an almost identical structure of a branched nonasaccharide with several free amino and carboxyl groups linked to a distal trisaccharide, called band A trisaccharide, whereas the *B. parapertussis* core comprises a heptasaccharide that lacks band A trisaccharide and two other monosaccharides (9). However, until now, the question of how the O antigens are linked to the core region remained unanswered. Here we present data that describe the complete structures of the *B. bronchiseptica* and *B. parapertussis* LPS carbohydrates.

EXPERIMENTAL PROCEDURES

NMR Spectroscopy—NMR spectra were recorded at 30 °C in D_2O on Varian UNITY INOVA 500, 600, or 800 instruments, using acetone as a reference for proton (2.225 ppm) and carbon (31.5 ppm) spectra. Varian standard programs COSY, NOESY (mixing time of 200 ms), TOCSY (spinlock time of 120 ms), HSQC, and gHMBC (long-range transfer delay of 100 ms) were used with digital resolution in the F2 dimension of <2 Hz/pt. Spectra were assigned using the Pronto program (10).

Monosaccharide Analysis—Hydrolysis was performed with 4 M trifluoroacetic acid (110 °C, 3 h). Monosaccharides were conventionally converted into alditol acetates and analyzed by gas chromatography on an Agilent 6850 chromatograph equipped with a DB-17 (30 m × 0.25 mm) fused silica column using a temperature gradient of 180–240 °C at 2 °C/min.

Mass Spectrometry—Electrospray ionization-MS spectra were obtained using a Micromass Quattro spectrometer in 50% MeCN with 0.2% HCOOH at a flow rate of 15 μl/min with direct injection. For capillary electrophoresis-MS analysis, a Prince CE system (Prince Technologies, The Netherlands) was coupled to a 4000 QTRAP mass spectrometer (Applied Biosystems/MDS Sciex, Canada). A sheath solution (isopropanol-methanol, 2:1) was delivered at a flow rate of 1.0 μl/min. Separations were obtained on an ~90-cm bare, fused silica capillary using 15 mM ammonium acetate, pH 9.0. An electrospray ionization voltage of 5 kV was used. Tandem mass spectra were obtained using an in-source fragmentation strategy with a decluster voltage of 300 V (11).

Chromatography—Anion exchange chromatography was performed on HiTrap Q column (5 ml; Pharmacia) in water (A) and 1 M NaCl (B) gradient from 0% B for 20 min and then linear gradient to 100% B with UV detection at 220 nm. Reverse phase chromatography was performed using C18 column (Aqua, 250 × 9 mm, Phenomenex) using a 0.1% trifluoroacetic acid-90% MeCN gradient (0% MeCN for the first 20 min, followed by a linear gradient to 100% MeCN over 1 h) with UV detection

* Work in the Preston laboratory is supported in part by a Natural Sciences and Engineering Research Council Discovery Grant. The costs of publication of this article were defrayed in part by the payment of page charges. This article must therefore be hereby marked "*advertisement*" in accordance with 18 U.S.C. Section 1734 solely to indicate this fact.

[1] To whom correspondence should be addressed: Inst. for Biological Sciences, National Research Council, 100 Sussex Dr., Ottawa, Ontario K1A 0R6, Canada. Tel.: 613-990-0832; Fax: 613-952-9092; E-mail: evguenii.vinogradov@nrc-cnrc.gc.ca.

[2] The abbreviations used are: LPS, lipopolysaccharide; HMBC, heteronuclear multiple bond connectivity; MS, mass spectrometry; HF, hydrogen fluoride; HPLC, high pressure liquid chromatography; FucNAc4NMe, 2-acetamido-4-methylamino-2,4,6-trideoxy-galactose; FucNAc4N, 2-acetamido-4-amino-2,4,6-trideoxy-galactose; GalNA, galactosaminuronic acid; GlcN, glucosamine; Hep, L-*glycero*-D-*manno*-heptose; Kdo, 3-deoxy-D-*manno*-octulosonic acid; ManNAc3NAcA, 2,3-diacetamido-2,3-dideoxy-mannuronic acid; GalNAc3NAcA, 2,3-diacetamido-2,3-dideoxy-galacturonic acid; GlcNAc3NAcA, 2,3-diacetamido-2,3-dideoxy-glucuronic acid.

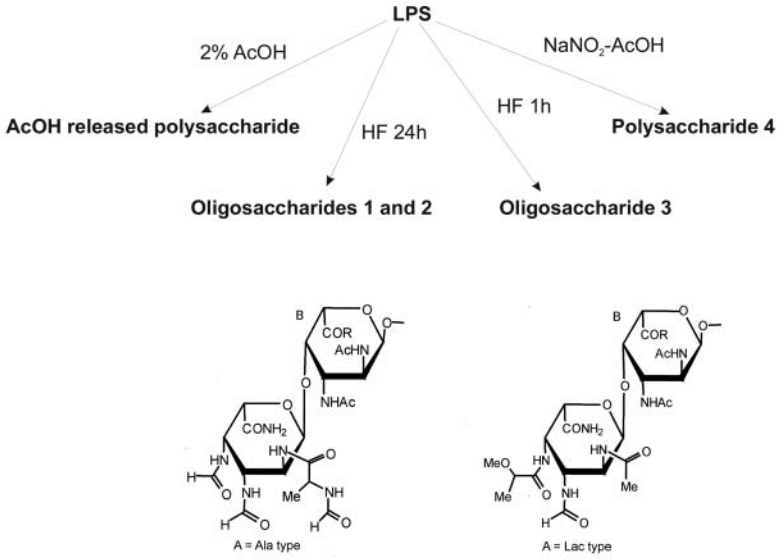

Non-reducing end groups of the *B. bronchiseptica* and *B. parapertussis* LPSs. R can be OH or NH_2.

Oligosaccharide **1** (A = Lac-type) and **2** (A = Ala-type)

A-4-(-α-GalNAc3NAcA-)$_n$-α-GalNAc3NAcAN-4-β-ManNAc3NAcAN-4-β-GlcNAc3NAcAN-4-α,β-GalNAc
Z MM X Y

Oligosaccharide **3**

K
α-GalNA-6┐

β-ManNAc3NAcA-3-β-FucNAc4NMe*-6-α-GlcNAc-4-β-ManNAc3NAcA-3-β-FucNAc4NMe*-6-α-GlcN-4-α-Glc-F
M' L' P M L J I

Oligosaccharide **4**

A-4-(-α-GalNAc3NAcA-)$_n$-α-GalNAc3NAcAN-4-β-ManNAc3NAcAN-4-β-GlcNAc3NAcAN-4-α-GalNAc-
D Z MM X Y

N
α-Hep-4┐

-4-β-ManNAc3NAcA-3-β-FucNAc4NMe*-6-α-GlcNAc-4-β-ManNAc3NAcA-3-β-FucNAc4NMe*-6-anhMan
M' L' P M L J

AcOH- released polysaccharides. The fragments in figure brackets are partially (N and K) or completely (P-M-L) absent from *B. parapertussis* LPS.

A-4-(-α-GalNAc3NAcA-)$_n$-α-GalNAc3NAcAN-4-β-ManNAc3NAcAN-4-β-GlcNAc3NAcAN-4-α-GalNAc-
D Z MM X Y

-4-β-ManNAc3NAcA-3-β-FucNAc4NMe*-{6-α-GlcNAc-4-β-ManNAc3NAcA-3-β-FucNAc4NMe*-}-
M' L' P M L

H
G α-GlcN-7┐ F
α-GlcA-2-α-Hep4*P**-3┐
-6-α-GlcN-4-β-Glc-4-α-Hep-5-anhKdo
{α-Hep-4}┘ J | I E C
N {α-GalNA-6}┘
K

FIGURE 1. **Schematic representation of the preparation of LPS derivatives and the structures of the isolated compounds.** To distinguish uronic acids from their amides the letter *n* is added at the end of abbreviated monosaccharide name for amides. * marks non-stoichiometric components; in the case of FucNAc4NMe* it refers to the Me group only.

at 220 nm. Size exclusion chromatography was performed on a Sephadex a G-15 column (1.6 × 80 cm) or Sephadex a G-50 column (2.5 × 80 cm) in pyridine-acetic acid buffer (4 ml of pyridine and 10 ml of acetic acid in 1 liter of water) using a refractive index detector (Waters).

Bacterial Strains and Cultures—*B. bronchiseptica* BAA-588 (RB50), 10580, and *B. parapertussis* 15311, 15989, and BAA-587 (12822) were obtained from ATCC. *B. bronchiseptica* 512 and 110H have been described previously (7). Bacteria were grown on Bordet-Gengou agar plates and then grown in Stainer-Scholte broth (12). Bacteria were harvested and frozen for LPS extraction. LPS extraction was performed using the phenol-water method as described (7).

Mild Hydrolysis of the LPS—The LPS (30–200 mg) were treated with 2% acetic acid at 100 °C for 3 h. The precipitate was removed by centrifugation, and soluble products were separated by gel chromatography on a Sephadex G-50 column. In most cases, a sharp peak of glucan was eluted from the column before the polysaccharide fraction of LPS was eluted. Polysaccharide and core fractions were collected and further purified by anion-exchange chromatography. Both polysaccharides and core gave two fractions on anion-exchange column, one eluting with the solvent front and another retained. Neutral fractions were dominant in core preparations, and acidic fraction dominated in the polysaccharide. Anion-exchange purification removed nucleic acid and protein contaminants; however, it introduced additional uncertainty in quantification of acidic groups.

HF Solvolysis of the LPS—LPS (50–150 mg) was dissolved in liquid anhydrous hydrogen fluoride (~5 ml) and kept at room temperature for either 1 or 24 h. HF was removed by evaporation on plastic Petri dishes. The residue was dissolved in water, precipitate was removed by centrifugation, and the soluble product chromatographed on Sephadex G-50 to yield a polysaccharide fraction (20–80 mg) and several oligosaccharide fractions in the case of the short solvolysis. The products were further separated by reverse phase chromatography. Oligosaccharides **1** and **2** were eluted in the middle region of the gradient. Oligosaccharides were analyzed by NMR, and similar fractions were combined (to give compound 3 shown in Fig. 1) and several other oligosaccharides that were not analyzed further in the current study.

Deamination of the LPS—LPS from strain 512 (100 mg) was dissolved in water (10 ml). $NaNO_2$ (200 mg) and AcOH (1 ml) were added, the solution was kept at room temperature for 24 h, lipids were removed by ultracentrifugation, and the solution was separated on a Sephadex G-50 column. Polysaccharide fractions were further separated by C18 HPLC as described above (yielding product **4** as shown in Fig. 1) and several other fractions.

RESULTS

Four strains of *B. bronchiseptica* (ATCC BAA-588 (RB50), ATCC 10580, 512, and 110H) and three strains of *B. parapertussis* (ATCC 15311, 15989, and BAA-587 (12822)) were used in the present study. The genome sequences of *B. bronchiseptica* RB50 and *B. parapertussis* 12822 have been recently generated and analyzed (5), allowing for the structural and genetic information to be linked.

Several derivatives of the LPS were prepared and are shown in Fig. 1. The NMR spectra of polysaccharides obtained after AcOH hydrolysis of the LPS were too complex to be interpreted directly (Fig. 2). This is a result of the presence of several structural variants differing in Kdo degradation products at the reducing end, partial methylation of 4-aminogroup of FucNAc4N, and partial phosphorylation of one Hep residue.

The O chain of *Bordetella* LPS is a polymer of 2,3-diacetamido-2,3-dideoxy-α-galacturonic acid. Glycosidic linkages of this monosaccharide are stable to treatment with anhydrous HF. Thus HF treatment was used to obtain the product with the first HF-susceptible monosaccharide at the reducing end. Prolonged treatment of all the LPS with anhydrous HF (24 h, 25 °C) led to the cleavage of glycoside bonds between all sugars except those between 2,3,4-trideoxy-2,3,4-triacylamino-α-galacturonamides, which are present at the non-reducing ends of the O chains (8), and of the 2,3-diacetamido-2,3-dideoxyuronic acids that comprise the repeating unit of the O chains. Following the removal of HF the products were desalted on Sephadex G-50 columns and the oligosaccharides were further purified by C18 reverse phase chromatography. This yielded large oligosaccharides that differed between strains in the terminal residues: the "Lac type" from strains RB50 and 512 (denoted structure **1** in Fig. 1) or the "Ala type" from strains 110H, 10580, 15311, 15989, and 12822 (denoted structure **2** in Fig. 1). These oligosaccharides include the complete O chains of the respective LPS, the monosaccharides at the non-reducing ends, and several additional monosaccharides proximal to the reducing end previously not characterized as part of the O chain. The oligosaccharides derived from different strains also differed in the degree of amidation of uronic acids, as will be discussed below.

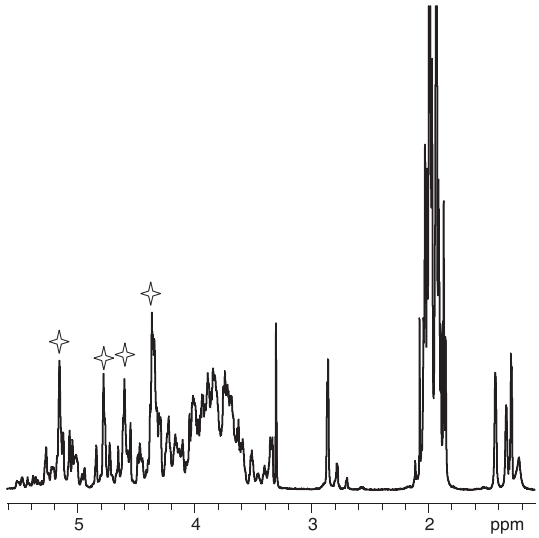

FIGURE 2. **^{1}H NMR spectrum of the AcOH-released polysaccharide of *B. bronchiseptica* RB50.** Signals marked with *stars* derive from α-GalNAc3NAcA residues of the O-chain.

A set of two-dimensional NMR spectra (COSY, TOCSY, NOESY, HSQC, HMBC) of the oligosaccharides obtained from each strain was recorded, and all proton and carbon signals were assigned (Table 1, Fig. 3). This revealed the expected oligomers of 2,3-diacetamido-2,3-dideoxy-α-galactopyranosyluronic acid with previously described (8) non-reducing end groups (Fig. 1). However, an additional three monosaccharide residues of 2,3-diacetamido-2,3-dideoxy-β-glucuronic acid, 2,3-diacetamido-β-2,3-dideoxy-mannuronic acid, and α,β-*N*-acetylgalactosamine at the reducing end were also identified. Thus oligosaccharides **1** and **2** (Fig. 1) were released from the LPS by the cleavage of the glycosidic linkage of GalNAc with HF. The presence of the GalNAc was confirmed by gas chromatography-MS analysis of alditol acetates; other monosaccharides could not be detected by chemical analysis and were identified only by NMR spectroscopy.

The relative configurations of the constituent monosaccharides were identified on the basis of vicinal proton coupling constants and ^{13}C NMR chemical shifts, which were in agreement with the standard values for each monosaccharide. Anomeric configurations were deduced from the $J_{1,2}$ coupling constants and chemical shifts of H-1, C-1, and C-5 signals as well as observation of intra-residue nuclear Overhauser

TABLE 1

Selected NMR data (δ, ppm)

Compound **1** was obtained from *B. bronchiseptica* RB50 LPS. Signals listed over / sign belong to the residues of the same type at different positions along the polymeric chain. L+Me residue refers to the 4-*N*-methyl-FucNAc4N; L−Me is FucNAc4N. Data shown in Table 1 were obtained at 40 °C, pH ~5.

Unit, compound	Nucleus	H/C 1	H/C 2	H/C 3	H/C 4	H/C 5	H/C 6	H/C 6′/Me
A, 1	H	5.23	4.22	4.53	4.83	4.58		
	C	98.8	48.8	46.9	49.7	71.3		
B α-GalNAc3NAcA, 1	H	5.20	4.47	4.36	4.59	4.67		
	C	97.5	47.6	49.5	75.2	71.5		
D α-GalNAc3NAcA acids, 1	H	5.16/5.17	4.35/4.38	4.36	4.63	4.86		
	C	96.5/98.1	47.5/47.1	49.5	76.0	70.5/70.9	172.2	
D α-GalNAc3NAcAN amides, 1	H	5.16/5.17	4.35/4.38	4.36	4.63	4.59		
	C	96.5/98.1	47.5/47.1	49.5	72.6	70.8/71.4	174.0	
I/I′ α-Glc-F, 3	H	5.60/5.69	3.62/3.66	3.92	3.66	4.09	3.82	3.87
	C		72.0/72.2	73.8	77.2	71.7	68.3	
J/J′ α-GlcN, 3	H	5.55/5.52	3.28	3.78	3.37	3.75	3.68	4.11
	C		55.3	70.4	70.5	73.0	69.7	
J α-GlcN, Rb50 PS	H	5.55/5.51	3.38	3.97	3.66	3.85	4.10	3.94
	C	98.4	57.8	70.9	78.9	71.6	68.1	
K α-GalNA, 3	H	5.25	3.51	4.13	4.32	4.47		
	C	96.8	51.7	67.5	70.2	72.5	173.7	
P α-GlcNAc, 3	H	5.02	3.70	3.60	3.37	3.70	3.80	3.99
	C	98.0	54.6	71.5	70.5	71.9	68.8	
P α-GlcNAc, Rb50 PS	H	5.08	3.78	3.66	3.43	3.77	3.86	4.03
	C	97.8	54.3	71.4	70.4	71.7	68.7	
M β-ManNAc3NAcA, 3	H	5.00	4.25	4.21	3.86	3.86		
	C	101.0	52.5	54.4	71.4	79.3	175.3	
M′ β-ManNAc3NAcA, 3	H	5.03	4.38	4.04	3.63	3.92		
	C	101.0	52.1	54.3	67.1	79.3	175.3	
L+Me β-FucNAc4NMe, 3	H	4.48	3.72	4.09	3.69	3.98	1.40	2.82
	C	102.7	51.8	79.4	63.5	69.1	17.3	36.7
L−Me β-FucNAc4N, 3	H	4.48	3.78	4.09	3.80	3.98	1.30	
	C	102.7	51.5	79.0	54.6	68.6	16.7	
L′+Me β-FucNAc4NMe, 3	H	4.52	3.72	4.12	3.72	3.98	1.40	2.86
	C	102.7	51.8	79.4	63.5	69.1	17.3	36.7
L′-Me β-FucNAc4N, 3	H	4.52	3.78	4.12	3.83	3.98	1.30	
	C	102.7	51.5	79.0	54.7	68.0	16.7	
Z α-GalNAc3NAcAN, 1	H	5.09	4.35	4.23	4.56	4.31		
	C	98.7	51.0	49.5	72.8	71.0	174.2	
Z α-GalNAc3NAcAN, Rb50 PS	H	5.15	4.34	4.26	4.58	4.34		
	C	98.6	47.3	49.3	72.7	70.9		
MM β-ManNAc3NAcAN, 1	H	4.76	4.37	4.22	3.96	4.06		
	C	100.8	51.9	53.0	73.9	77.2		
MM β-ManNAc3NAcAN Rb50 PS	H	4.76	4.38	4.20	3.93	4.00		
	C	100.7	51.8	53.1	79.2	71.6		
X β-GlcNAc3NAcAN, 1	H	4.89	3.89	4.00	3.84	3.99		
	C	103.0	54.4	54.5	79.1	75.6	173.7	
X β-GlcNAc3NAcAN, Rb50 PS	H	4.88	3.88	4.02	3.86	4.01		
	C	102.9	54.3	54.2	79.0	75.3		
α-Y α-GalNAc, 1	H	5.18	4.03	4.01	4.13	4.07	3.73	
	C	92.3	51.7	68.8	77.1	71.3	62.3	
β-Y β-GalNAc, 1	H	4.60	3.78	3.80	4.06	3.65	3.73	
	C	96.7	55.1	72.6	76.1	75.6	62.3	
Y α-GalNAc, Rb50 PS	H	5.11	4.03	3.95	4.13	4.00	3.70	3.75
	C	102.2	50.5	67.9	80.1	71.6	62.2	
M, M′ β-ManNAc3NAcA Rb50 PS	H	5.04/5.06	4.32	4.26	3.91	4.07		
	C	100.8	52.4	54.2	71.1	79.2		
L+Me β-FucNAc4NMe Rb50 PS	H	4.60	3.85	4.17	3.74	4.04	1.45	2.89
	C	101.8	51.4	79.0	63.6	69.5	17.2	36.7
L−Me β-FucNAc4N Rb50 PS	H	4.59	3.77	4.2	3.86	4.05	1.36	
	C	102.4	51.6	78.5	54.6	69.5	16.6	
Lac	H		3.95	1.30				3.33
	C	177.7	78.6	19.0				57.9

effects for β-pyranosides (Fig. 1, residues *β-Z*, *MM*, and *X*). Connections between the monosaccharides were determined on the basis of the inter-residue nuclear Overhauser effects (Fig. 3) and heteronuclear multiple bond connectivity (HMBC) correlations (the HMBC correlations are not presented but they are all as expected for the structure). All interglycoside correlations expected for structures **1** and **2** were observed. Thus, in addition to the previously known structures of the repeating units and non-reducing end groups, the polysaccharides con-

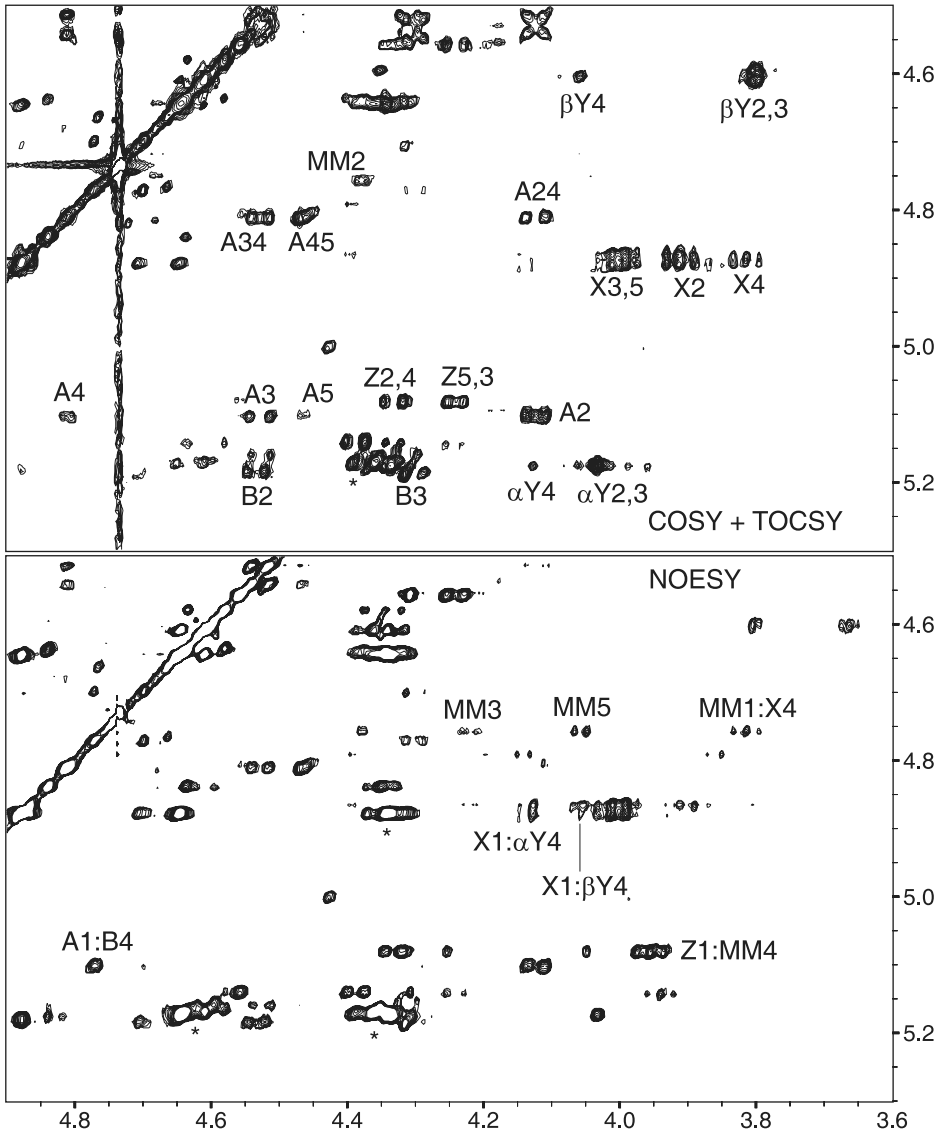

FIGURE 3. **Fragments of two-dimensional NMR spectra of oligosaccharide 2, obtained from *B. parapertussis* 15311.** *Top*, TOCSY; *bottom*, NOESY with labeled transglycoside correlations and intra-ring signals of residue MM. * marks signals derived from α-GalNAc3NAcA units of the polysaccharide chain.

tain the following trisaccharide sequence at the reducing end: PS-4-β-ManNAc3NAcAN-4-β-GlcNAc3NAcAN-4-GalNAc. This sequence was present in the oligosaccharides obtained from all strains.

Determination of the Degree of Amidation of Diacetamidouronic Acids—The electrospray mass spectra of compounds **1** and **2** (Fig. 4) were consistent with the presence of oligomers of 2,3-diacetamido-2,3-dideoxyhexuronic acid with the non-reducing terminal structures shown in Fig. 1. The molecular mass distributions indicated that chains with 11–12 α-GalNAc3NAcA residues were the most abundant for each O antigen. For example, in the spectrum of *B. bronchiseptica* 10580 shown in Fig. 4 the peak at 4158.3 corresponds roughly to 12 α-GalNAc3NAcA residues with the respective reducing and non-reducing end monosaccharides (expected average mass 4165.7 Da).

However, the calculated masses for these structures containing all uronic acids (not counting the 2,3,4-triaminouronic acid terminal residue at the non-reducing end, which was always present in the amide form) were 3–8 units higher than those observed for each peak in the mass spectra. This pointed to the amidation of the respective number of uronic acid residues. Detailed analysis of the peaks in the mass spectra (Fig. 4, *insert*) showed that they are broad and consist of many components, which is the result of an overlap between the isotopic distributions and ions derived from the molecular species with different degrees of amidation. Thus, each O antigen comprises a mixture of the molecules with different numbers of amidated residues, and it was only possible to determine the average number of amidated residues. Oligomers of different lengths showed variable deviation from the calculated mass of the non-amidated products, as shown in Fig. 5, with maximum deviation observed for polymers of 12 α-GalNAc3NAcA units in all strains. This peak in amidation of the most abundant polymer length may reflect a specific feature of the biosynthesis of these polymers.

To confirm the presence of amidated residues and to possibly determine their position within the chain, the pH dependence of NMR chemical shifts of the oligosaccharides **1** and **2** was analyzed using HSQC spectra. The spectra were recorded at two different pH, first without adjustment (pH ~5) and then after addition of 5 μl of 20% ND_4OD (pH ~9) in order to observe the pH-induced shift of H/C-4 and H/C-5 signals of non-amidated uronic acids. This experiment (Fig. 6) showed that the signals from residues X, MM, and Z (Fig. 1, *Z* is the first α-GalNAc3NAcA residue of the O chain) did not change positions, and hence these three residues were always amidated. The H/C-4 and H/C-5 signals from the rest of the α-GalNAc3NAcA residues fell into two groups: one that sharply changed their position and thus belonged to free acids and the other that did not because of amidation. It was not possible to quantify how many of the signals shifted. Thus, combined

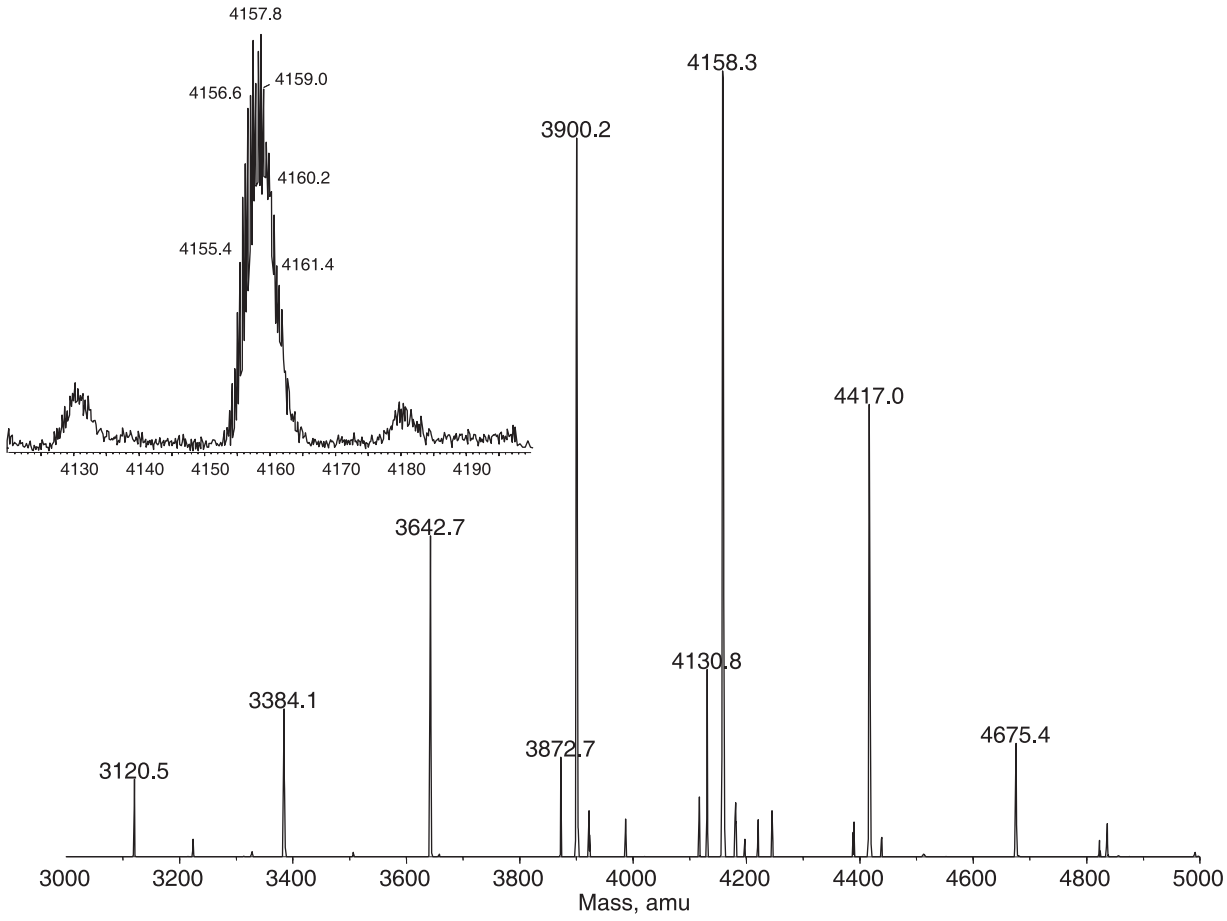

FIGURE 4. **Electrospray ionization-MS spectrum of oligosaccharide 2, obtained from *B. bronchiseptica* 10580 LPS.** Expanded view of a peak at 4158.3 shows its complex structure.

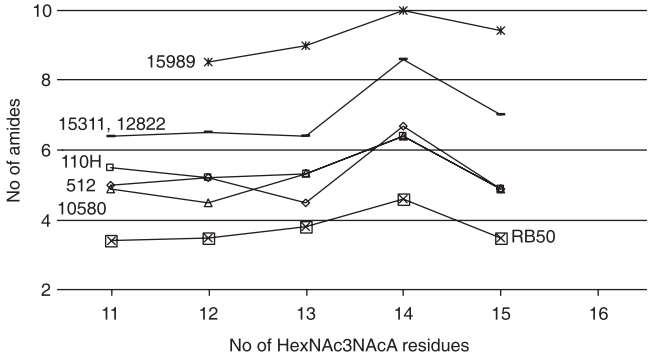

FIGURE 5. **Mass differences between the calculated mass for a structure containing only non-amidated diacetamidouronic acids and the observed values (MS) for oligosaccharides 1 and 2.**

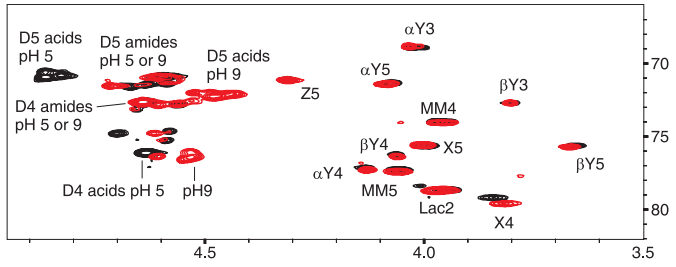

FIGURE 6. **Fragment of the HSQC spectra (ring CH-OH signals) of oligosaccharide 1, obtained from *B. bronchiseptica* strain Rb50, recorded at pH 5 (*black*) and pH 9 (*red*).** Signals from α-GalNAc3NAcA of the PS chain are labeled *D*.

NMR and MS data indicated complete amidation of the residues X, MM, and Z and the presence of several additional amidated residues in the O chain.

MS/MS experiments were used to further visualize the presence of free and amidated uronic acids (Fig. 7). Secondary ions corresponding to glycosylations of 2,3-diacetamido-hexuronic acids in free acid or amide forms (*m*/*z* 258 and 257, respectively) were observed, as well as ions of their dimers and trimers. The relative intensity of the ions indicated the presence of blocks of amides and blocks of acids, whereas mixed amide/acid ions were less abundant. This indicated the presence of the three amides in a row (residues Z-MM-X) and the dominance of free acids in the repeating units. Ions of the terminal residue A (Lac-type, 328.3 Da, and Ala-type, 327.3 Da) were present in the spectra of oligosaccharides **1** and **2,** respectively, as well as ions of dimers of residues A and B (the penultimate monosaccharide). The peaks derived from the A-B disaccharides of the different strains differed in mass depending on whether B was present as an acid or an amide. Residue B was in amide form in all *B. parapertussis* strains but in acid form in all *B. bronchiseptica* strains (Table 2), in agreement with the increased level of amidation observed by MS in *B. parapertussis* strains 12822, 15311, and 15989 (Fig. 5). The amidation of residue B was observed in ^{1}H NMR spectra: the H-1 signal of residue A was sensitive to the acid/amide transition in residue B, shifting by ~0.03 ppm (for Ala-type residue A) or 0.1 ppm (for Lac-type residue A) to high field due to this change (data not shown).

Analysis of the Connection between Oligosaccharides 1 and 2 and the Core—Treatment of *B. bronchiseptica* RB50 LPS with HF for a short time (1 h, 25 °C) led to the formation of a large number of oligosaccha-

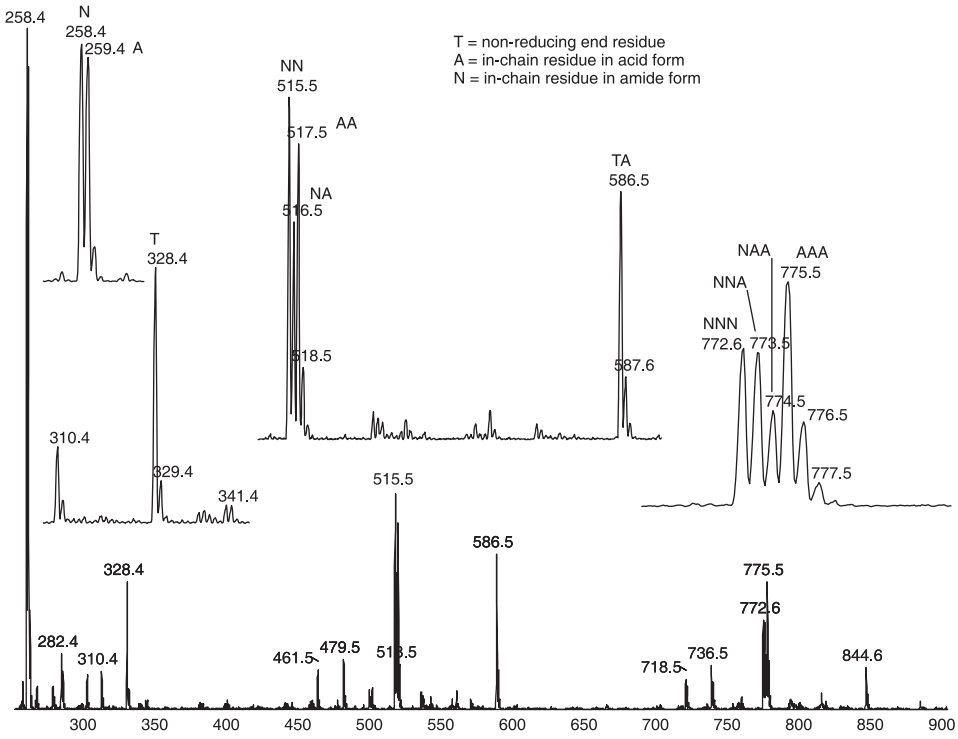

FIGURE 7. **MS/MS fragmentation spectra of oligosaccharide 2, obtained from *B. bronchiseptica* 110H LPS.**

rides, which were separated by reverse phase HPLC. Determination of the structures of these products led to the discovery of oligosaccharide **3** (Fig. 1). It was analyzed by NMR (Table 1) and MS. Complete assignment of all NMR ^{1}H and ^{13}C signals led to the structure presented in Fig. 1. Important information obtained from this structure was the presence of two copies of β-ManNAc3NAcA-3-β-FucNAc4NMe* (both FucNAc4N residues can have either a free or methylated amino group at C-4). The NMR-based identification was supported by the MS observation of the expected masses of this oligosaccharide: 1638.6 Da (two methyl groups), 1624.6 Da (one methyl group), and 1610.6 Da (non-methylated). Further analysis (see below) demonstrated that oligosaccharide **3** was substituted by the O chain (oligosaccharides **1** and **2**) at O-4 of ManNAc3NAcA (Fig. 1, *residue M′*) in the LPS.

B. bronchiseptica RB50 LPS was subjected to deamination in an attempt to cleave the fragment ending at GlcN (Fig. 1, *residue J*) from the inner core. This treatment yielded several products due to additional reactions of $NaNO_2$ with free amino groups at C-4 of FucNAc4N or of FucNAc4NMe. All residues of FucNAc4N with a free amino group at C-4 were destroyed by deamination, but those with methylated amino groups were converted into O=N-O-derivatives at FucNAc4N N-4, as previously observed (13). The products were separated by reverse phase HPLC, and the main product (Fig. 1, *structure 4*) was isolated.

Its structure was analyzed using NMR and MS. In the NMR spectra the signals from all of the components of oligosaccharide **1** were identified. The GalNAc residue (Fig. 1, *residue Y*, the reducing end monosaccharide in oligosaccharides **1** and **2**) had the α-configuration. It was linked to O-4 of the diacetamido-β-mannuronic acid, residue M′. The fragment M′-L′-P-M-L was the same as determined for oligosaccharide **3**, except that N-4 of both FucNAc4NMe residues (L and L′) was modified by substitution with O=N-O-. This substitution caused a low field shift of the H-4 signal of FucNAc4NMe by ~1 ppm (data not shown). At the reducing end of oligosaccharide **4** was 2,5-anhydromannose, a deamination product of GlcN (residue J). Otherwise all monosaccharides had the expected coupling constants and signal positions consistent with the overall structure depicted in Fig. 1.

TABLE 2
Structure of the non-reducing end of the polysaccharides
The presence of the residue B as an acid or amide must not be treated as absolutely true; traces of the opposite variant can be seen in some samples.

Strain	Residue A	Residue A	Residue B-acid	Residue B-amide
	Lac-type	Ala-type		
Bb 512	+		+	
Bb 110H		+	+	
Bb 10580		+	+	
Bb RB50	+		+	
Bpp 15311		+		+
Bpp 15989		+		+
Bpp 12822		+		+

The most important information obtained from the analysis of oligosaccharide **4** was that it contained the band A trisaccharide (residues P-M-L), substituted by a similar trisaccharide consisting of the residues M′ and L′ but with an α-GalNAc (residue Y) instead of α-GlcNAc. The NMR signals from H/C-6 of residues P (GlcNAc) and J (anh-Man, derived from GlcN) were separated in the spectra of oligosaccharide **4**, allowing differentiation between fragments M-L (attached to J) and M′-L′ (attached to P), which were indistinguishable in the spectra of the intact polysaccharides. Nuclear Overhauser effects and heteronuclear multiple bond connectivity correlations between H-1 of residue L and C-6 of residue J and between H-1 of residue L′ and C-6 of residue P were observed, confirming the structure shown in Fig. 1.

Thus, oligosaccharide **4** was a combination of oligosaccharides **1** and **3**, containing both the O chain and a fragment of the core. Using these data the entire structure of the outer part of *B. bronchiseptica* strain Rb50 LPS could be assembled. This in turn facilitated the interpretation of spectra derived from all other strains.

Analysis of the AcOH-released Polysaccharides—Structural data generated from analysis of oligosaccharide **4** made it possible to analyze the structure of the AcOH-released polysaccharide of *B. bronchiseptica* RB50. Most of the signals in these extremely complex spectra were assigned (partly presented in Table 1). No additional components and no contradiction with the structure inferred from the analysis described

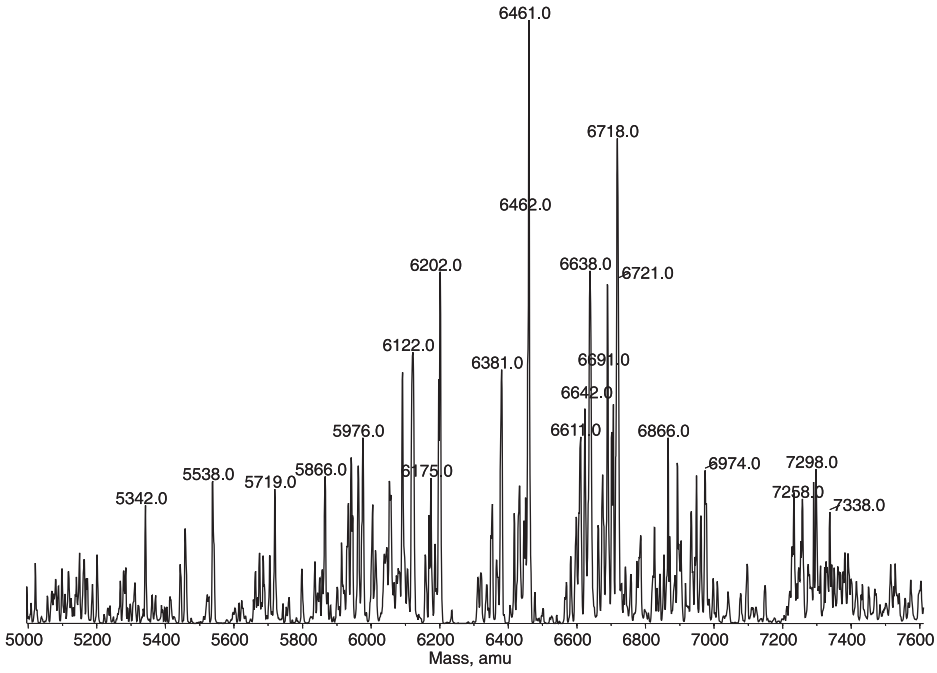

FIGURE 8. **Electrospray ionization mass spectrum of *B. bronchiseptica* RB50 PS obtained by AcOH hydrolysis of the LPS.**

above were observed. The capillary electrophoresis-MS spectrum of this polysaccharide (Fig. 8) contained groups of peaks, separated by 258 units (corresponding to diacetamidohexuronic acid). The most intense peak at 6461 Da corresponded to the composition Hex_1 Hep_3 $HexA_1$ $HexNA_1$ $HexN_4$ $HexN2A_{15}$ $HexN3A_1$ Kdo_1 $dHexN2_2$ $AcOH_{33}$ $Formyl_1$ P_1 Lac_1 $MeOH_3$ with four amides and Kdo in the anhydro form and was consistent with the proposed structure. Minor peaks in each group were due to dephosphorylation and incomplete methylation.

Analysis of spectra of the AcOH-released polysaccharides from the other strains of *B. bronchiseptica* showed the presence of this structure with the same (strain 512) or different (strains 10580 and 110H) non-reducing ends. However, as was expected from previously published data on the structure of *B. parapertussis* LPS core (9), *B. parapertussis* polysaccharide had different structures: the fragment P-M-L was absent. Thus, residue L′ was linked directly to the O-6 of GlcN (residue J). The Hep (N) and GalNA (K) residues were present in small amounts (~25%) and were only found in core substituted with the O chain. Only Ala-type non-reducing ends were found in *B. parapertussis* O chains. These were the only differences observed between the *B. parapertussis* and *B. bronchiseptica* structures. Mass spectra of *B. parapertussis* AcOH-released polysaccharides were of poor quality, probably due to additional heterogeneity associated with the variable presence of the residues N and K.

DISCUSSION

B. pertussis, *B. parapertussis*, and *B. bronchiseptica* share many aspects of pathogenicity and yet have distinct host ranges and cause different pathologies in their hosts (2). This is probably related to the differences in the way these bacteria interact with their hosts, which in turn is likely to be affected by the bacterial surface components. The LPS of these bacteria show many similarities (14) but display a number of important differences, as demonstrated here. For example, unlike *B. bronchiseptica* and *B. parapertussis*, *B. pertussis* does not express an O antigen due to deletion of the *wbm* locus that contains the O antigen biosynthesis genes (15). Furthermore, *B. parapertussis* and *B. bronchiseptica* both express similar O antigens but possibly play different roles during infection (16).

Core—Here we have shown a missing part of the carbohydrate backbone of *B. bronchiseptica* and *B. parapertussis* LPS that, along with previous publications, describes the complete LPS structures of these bacteria. We have confirmed previous observations that the cores of these LPS are conserved in respect to sugar composition and their arrangements. The *B. bronchiseptica* core is identical to that described for a strain of *B. pertussis* (17). The *B. parapertussis* LPS core differs in two aspects. We have confirmed that it is deficient in the distal trisaccharide that gives rise to the well known SDS-PAGE band A of Bordetellae LPS. This trisaccharide is biosynthesized by the *wlb* gene products (18). *B. parapertussis* contains a *wlb* locus, and thus the absence of the trisaccharide is not simply due to the absence of the necessary biosynthetic genes. Previously, the absence of band A LPS from *B. parapertussis* was hypothesized to be due to a point mutation in the *wlbH* gene thought to encode the GlcNAc transferase that adds this terminal sugar (residue P) to form band A LPS (19, 20). Until now it was thought that the O antigen was attached to the core by a linkage to the second sugar of the trisaccharide (residue M) and that attachment of either GlcNAc or O antigen to residue M determined the biosynthesis of band A LPS or O antigen containing LPS. The *wlbH* mutation was proposed to reduce or eliminate WlbH activity such that all of the LPS core was substituted by the O antigen, resulting in the lack of band A LPS that is observed with *B. parapertussis*. Our data demonstrate that band A trisaccharide (L-M-P) is completely absent from *B. parapertussis*. The reason is at present unclear. Mutation of *wlbH* in *B. pertussis* results in the addition of the first two sugars of the trisaccharide to the core (20), and thus it is not necessary for the entire trisaccharide to be present for transfer from undecaprenol to the core.

The *B. parapertussis* core also differs from those of *B. bronchiseptica* and *B. pertussis* in that the terminal heptose (residue N) and the terminal GalNA (residue K) residues are not present on all molecules. Again, the genetic basis for this variability is unclear. The genes encoding the heptosyltransferase that adds this heptose to the core (genes BB3923/BPP3474/BP2487 of the annotated genome sequences) (5) are present[3]

[3] A. Preston, unpublished observation.

and apparently intact in *B. parapertussis*. Also, the *B. parapertussis* core locus (21) that presumably contains the gene encoding the GalNA transferase does not contain any obvious differences from the *B. bronchiseptica* and *B. pertussis* loci to explain the variable addition of these sugars in *B. parapertussis.* Putative regulatory mechanisms that influence core structure are currently being investigated.

An interesting question is why the *B. parapertussis* core differs from those of the other Bordetellae. This might be due to host immune selective pressure. *B. parapertussis* evolved from a *B. bronchiseptica* lineage very recently and at a time when *B. pertussis* was already present in the same host niche. Thus, *B. parapertussis* evolved in the presence of anti-*B. pertussis* immunity, and this may have selected for *B. parapertussis* that do not express the same antigens as *B. pertussis* (discussed in Ref. 22). That band A LPS is highly immunogenic supports this theory (23), and this may indicate that the terminal heptose and GalNAc residues are also targets of host anti-*B. pertussis* immunity.

O Antigen—We have elucidated the linkage of the O antigen to the core, which had remained elusive until now. In *B. bronchiseptica* the O antigen is attached to GlcNAc of the band A trisaccharide. In *B. parapertussis*, in the absence of this trisaccharide it is attached to GlcN of the core (residue J). The O antigen-core ligases, encoded by BB3922/BPP3473,[3] in these bacteria are nearly (97%) identical at the amino acid level. Thus, either the amino or *N*-acetyl substitutions of these acceptors are not part of the substrate recognition domain of the ligase or it has a relaxed substrate specificity that enables it to transfer the O antigen to either GlcNAc or to GlcN. This ligase also transfers band A trisaccharide to the core (in all three species).[3] The same sugar, -β-FucNAc4NMe, is linked to the core in the case of both band A (residue L) and O antigen addition (L′). In both cases the acceptor sugar is again either GlcNAc (O antigen addition in *B. bronchiseptica*) or GlcN (Band A trisaccharide addition in *B. bronchiseptica* or O antigen addition in *B. parapertussis*), and thus the linkages involved in each of these cases are very similar.

Importantly, this study identified that *Bordetella* O antigen is linked to the core via a novel five-sugar linker that was not identified in previous studies. The linker is the same in *B. bronchiseptica* and *B. parapertussis*. It contains a structure similar to the band A trisaccharide, but in which α-GalNAc replaces α-GlcNAc, and a β-GlcNAc3NAcAN and a β-ManNAc3NAcAN residue. The fact that this linker is found only in O antigen-containing LPS and not in *B. pertussis* that does not express O antigen suggests that it is a part of the O antigen and not an extension of the core. Thus we propose that the O antigen repeats are added to this linker on an undecaprenol carrier and that this is added *en bloc* to the core.

The presence of this linker correlates with the complexity of the genetics of O antigen biosynthesis in Bordetellae. The *wbm* loci of *B. bronchiseptica* RB50 and *B. parapertussis* 12822 contain 24 genes, many of which are almost identical between the loci, consistent with the fact that their O antigens comprise the same linker region and the same homopolymeric repeat (15). The central regions of the loci differ, and this was thought to encode the functions that synthesize the modifications of the terminal repeat residue. That strains RB50 and 12822 contain different terminal residues (Table 2) supports this proposal. The functions of most of the *wbm* genes are unknown, but the locus appears too big for the synthesis of the -α-GalNAc3NAcA- homopolymer. We thus propose that some *wbm* genes function to synthesize the linker. Several putative glycosyltransferases appear to be encoded by the *wbm* locus (21), and these might function to assemble the linker. The biological function of this unusual linker is unclear at present.

Both types of terminal modifications were identified in the *B. bronchiseptica* genus, whereas all *B. parapertussis* strains studied here contain the Ala-type modification (Table 2). This is consistent with *B. bronchiseptica* comprising genetically variable strains whereas *B. parapertussis* comprises strains with little genetic variation, probably reflecting the recent formation of this species (24, 25). The relation of these modifications to infection is unknown.

Amidation of O Antigen Residues—We found that some of the uronic acids in the O chain are amidated. Interestingly, only some residues appear to be consistently amidated, for example the β-ManNAc3NAcAN and β-GlcNAc3NAcAN residues of the linker (residues MM and X) and the first GalNAc3NAcA residue of the repeat (residue Z). The positions of the amidated residues within the O chain remain unknown. Also of interest is that amidation of the penultimate residue (residue B) appears to be species specific as it is amidated in all the *B. parapertussis* strains studied but is not completely amidated in all the *B. bronchiseptica* strains. The amidation changes the net charge of the O antigen and thus can alter its interaction with the environment of the bacterium and possibly the recognition of the O antigen by the host immune system.

This study reveals interesting differences between LPS of Bordetellae and provides a basis for studies of their pathogenesis and evolution. The identification of the linker that joins the O antigen to the core is an important finding for elucidating the genetic basis of LPS biosynthesis in these pathogens. A recent report identified that some *B. bronchiseptica* strains may synthesize different O antigens (25), and the work presented here will provide a basis for comparative analysis of the LPS of these strains.

Acknowledgments—We thank Dr. M. B. Perry (NRC Canada) for LPS samples and general support of this work and Dr. J. B. Robbins and R. Schneerson (NIH, Bethesda, MD) for reviewing the manuscript. The NMR spectra at 800 MHz were obtained at the Varian Unity Inova spectrometer of the Danish Instrument Center for NMR Spectroscopy of Biological Macromolecules.

REFERENCES

1. Stevenson, A., and Roberts, M. (2003) *FEMS Immunol. Med. Microbiol.* **37,** 121–128
2. Mattoo, S., and Cherry, J. D. (2005) *Clin. Microbiol. Rev.* **18,** 326–382
3. Woolfrey, B. F., and Moody, J. A. (1991) *Clin. Microbiol. Rev.* **4,** 243–255
4. Gueirard, P., Weber, C., Le, C. A., and Guiso, N. (1995) *J. Clin. Microbiol.* **33,** 2002–2006
5. Parkhill, J., Sebaihia, M., Preston, A., Murphy, L. D., Thomson, N., Harris, D. E., Holden, M. T., Churcher, C. M., Bentley, S. D., Mungall, K. L., Cerdeno-Tarraga, A. M., Temple, L., James, K., Harris, B., Quail, M. A., Achtman, M., Atkin, R., Baker, S., Basham, D., Bason, N., Cherevach, I., Chillingworth, T., Collins, M., Cronin, A., Davis, P., Doggett, J., Feltwell, T., Goble, A., Hamlin, N., Hauser, H., Holroyd, S., Jagels, K., Leather, S., Moule, S., Norberczak, H., O'Neil, S., Ormond, D., Price, C., Rabbinowitsch, E., Rutter, S., Sanders, M., Saunders, D., Seeger, K., Sharp, S., Simmonds, M., Skelton, J., Squares, R., Squares, S., Stevens, K., Unwin, L., Whitehead, S., Barrell, B. G., and Maskell, D. J. (2003) *Nat. Genet.* **35,** 32–40
6. Caroff, M., Karibian, D., Cavaillon, J. M., and Haeffner-Cavaillon, N. (2002) *Microbes. Infect.* **4,** 915–926
7. Di Fabio, J. L., Caroff, M., Karibian, D., Richards, J. C., and Perry, M. B. (1992) *FEMS Microbiol. Lett.* **76,** 275–281
8. Vinogradov, E., Peppler, M. S., and Perry, M. B. (2000) *Eur. J. Biochem.* **267,** 7230–7237
9. Caroff, M., Aussel, L., Zarrouk, H., Martin, A., Richards, J. C., Therisod, H., Perry, M. B., and Karibian, D. (2001) *J. Endotoxin. Res.* **7,** 63–68
10. Kjaer, M., Andersen, K. V., and Poulsen, F. M. (1994) *Methods Enzymol.* **239,** 288–308
11. Li, J., Wang, Z., and Altman, E. (2005) *Rapid Commun. Mass Spectrom.* **19,** 1305–1314
12. Stainer, D. W., and Scholte, M. J. (1970) *J. Gen. Microbiol.* **63,** 211–220
13. Vinogradov, E. V., and Perry, M. B. (2000) *Eur. J. Biochem.* **267,** 2439–2446
14. Harvill, E. T., Preston, A., Cotter, P. A., Allen, A. G., Maskell, D. J., and Miller, J. F. (2000) *Infect. Immun.* **68,** 6720–6728

15. Preston, A., Allen, A. G., Cadisch, J., Thomas, R., Stevens, K., Churcher, C. M., Badcock, K. L., Parkhill, J., Barrell, B., and Maskell, D. J. (1999) *Infect. Immun.* **67,** 3763–3767
16. Burns, V. C., Pishko, E. J., Preston, A., Maskell, D. J., and Harvill, E. T. (2003) *Infect. Immun.* **71,** 86–94
17. Caroff, M., Brisson, J., Martin, A., and Karibian, D. (2000) *FEBS Lett.* **477,** 8–14
18. Allen, A., and Maskell, D. (1996) *Mol. Microbiol.* **19,** 37–52
19. Allen, A. G., Thomas, R. M., Cadisch, J. T., and Maskell, D. J. (1998) *Mol. Microbiol.* **29,** 27–38
20. Preston, A., Thomas, R., and Maskell, D. J. (2002) *Microb. Pathog.* **33,** 91–95
21. Preston, A., and Maskell, D. (2001) *J. Endotoxin. Res.* **7,** 251–261
22. Bjornstad, O. N., and Harvill, E. T. (2005) *Trends Microbiol.* **13,** 355–359
23. Shahin, R. D., Hamel, J., Leef, M. F., and Brodeur, B. R. (1994) *Infect. Immun.* **62,** 722–725
24. Cummings, C. A., Brinig, M. M., Lepp, P. W., van de Pas, S., and Relman, D. A. (2004) *J. Bacteriol.* **186,** 1484–1492
25. Diavatopoulos, D. A., Cummings, C. A., Schouls, L. M., Brinig, M. M., Relman, D. A., and Mooi, F. R. (2005) *PLoS. Pathog.* **1,** e45

Complete Structures of *Bordetella bronchiseptica* and *Bordetella parapertussis* Lipopolysaccharides

Andrew Preston, Bent O. Petersen, Jens Ø. Duus, Joanna Kubler-Kielb, Gil Ben-Menachem, Jianjun Li and Evgeny Vinogradov

J. Biol. Chem. 2006, 281:18135-18144.
doi: 10.1074/jbc.M513904200 originally published online April 21, 2006
